Proceedings of the 9th International Conference on Structural Dynamics, EURODYN 2014
Porto, Portugal, 30 June - 2 July 2014
A. Cunha, E. Caetano, P. Ribeiro, G. Müller (eds.)
ISSN: 2311-9020; ISBN: 978-972-752-165-4

# Numerical and experimental investigation of a vibration system with non-ideal vibration source

Paulo J. P. Gonçalves[1], Marcos Silvera[1], Bento R. Pontes Jr.[1]
[1]Department of Mechaincal Eng., Faculty of Engineering of Bauru, State University of São Paulo,
Av. Eng. Luiz Edmundo C. Coube 14-01. Bauru, Brazil
email: paulo.jpg@feb.unesp.br, m.silveira@feb.unesp.br, brpontes@feb.unesp.br

ABSTRACT: An excitation force that is not influenced by the system's states is said to be an ideal energy source. In real situations, a direct and feedback coupling between the excitation source and the system must always exist. This manifestation of the law of conversation of energy is known as Sommerfeld Effect. In the case of obtaining a mathematical model for such system, additional equations are usually necessary to describe the vibration sources and their coupling with the mechanical system. In this work, a cantilever beam and a non-ideal electric DC motor that is fixed to the beam free end is analyzed. The motor has an unbalanced mass that provides excitation to the system proportional to the current applied to the motor. During the motor's coast up operation, as the excitation frequency gets closer to the beam first natural frequency and if the drive power increases further, the DC motor speed remains constant until it suddenly jumps to a much higher value (simultaneously the vibration amplitude jumps to a much lower value) upon exceeding a critical input power. It was found that the Sommerfeld effect depends on some system parameters and the motor operational procedures. These parameters are explored to avoid the resonance capture in Sommerfeld effect. Numerical simulations and experimental tests are used to help insight this dynamic behavior.

KEY WORDS: Sommerfeld Effect, Non-Ideal Energy Source

## 1 INTRODUCTION

Rotating machines suffer from unbalance and alignment problems that can lead to excessive levels of vibration, causing various undesirable problems and failures. All rotating machines are never perfectly balanced and therefore critical speeds must always exist. In summary, critical speed occurs when the shaft angular speed matches the shaft bending natural frequency.

According to reference [1], Laval was the first to perform an experiment with a steam turbine to observe that quick passage though critical speed would reduce significantly the levels of vibration when compared to steady state excitation.

This procedure would require a motor with enough power to be accelerated quickly in the range of resonance frequency. In some cases motors may have limited power to perform such operation and the angular velocity increases slowly such that the passage through resonance may be a problem.

Another class of problem related to unbalanced motors with limited power was discussed by Arnold Sommerfeld in 1902 [2]. He proposed an experiment of a motor mounted on a flexible wood table and observed that the power supplied to the motor was wasted in the form of table vibration, instead of been converted to angular velocity of the motor. This observation was used to explain a class of motors called non-ideal energy sources.

The interaction of non-ideal motors and flexible structures has been studied by many authors. A review of non-ideal Energy source is presented by references [1] and [3]. Eckert [4] presents a brief review of the problem investigate by Sommerfeld.

Ref [5] discusses the motion of an unbalanced rotor when passing through a resonance zone solved by the iteration method combined with the method of the direct separation of motions.

Dimentberg [6] presents a method to avoid resonance capture by switching on and off a mechanism to change the stiffness of an engine mount.

In this work, a motor mounted on a cantilever beam is studied. The system is modeled as motor mounted on a single degree of freedom spring-mass-damper oscillator. Experimental setup is used to validate the model. Results of the experimental test show agreement with the results obtained with numerical simulations.

## 2 SYSTEM MODELING

In the following sections, the equations of motion of an electrical motor attached to a structure are developed based on Hamilton's principle. The model is related to a physical system presented in the experimental section described hereafter.

### *2.1 Model Definition*

Figure 1 shows the system considered in this work, which is a cantilever beam and a concentrated mass positioned at its free end. Represented by $M_c$, the concentrated mass can take into account the mass of an electric motor, for instance. The motor has moment of inertia $J_0$ and is considered to be unbalanced, with unbalanced mass $m_r$ that rotates at a distance $r$ from the motor shaft center.


Figure 1. Cantilever beam with a concentrated mass and an unbalanced DC motor.

The beam is made of steel and its properties are defined by the Young's modulus $E$, the mass density $\rho$ , the length $L$ , the cross section area $S$ and the second moment of area $I$. For low amplitudes of oscillation, according to ref. [7], and if the higher order modes are neglected, it is possible to write a expression for the first bending natural frequency $\omega_0$ as

$$\omega_0 = \sqrt{\frac{3EI}{L^3(0.23\, m_b + M_c + m_r}} \tag{1}$$

Where $m_b = \rho SL$ is the mass of the beam.
The term $k = 3EI/L^3$ is the beam bending stiffness and can be used to define a simplified spring-mass-damper oscillator model shown in figure 2.

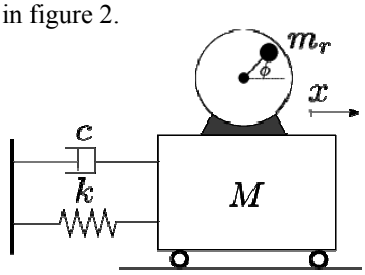


Figure 2. Representation of the system with a spring-mass-damper oscillator and a coupled DC motor with unbalanced mass.

The viscous damping coefficient is used to represent the energy loss in the system. The mass of this system can take into account the concentrated mass and the beam mass shown in figure 1, such that $M = (M_c + 0.23m_b)$. The cart displacement is define by $x$ and the motor angular position is represented by $\phi$.

## 2.2 *Energy Equations*

To apply Hamilton's principle, expressions for the kinetic and potential energy need to be written in terms of the unknown degrees of freedom.

The kinetic energy is straight-forward to write

$$T = \frac{1}{2}M\dot{x}^2 + \frac{1}{2}J_0\dot{\phi}^2 + \frac{1}{2}m_r(\dot{x}^2 + \dot{y}^2) \tag{2}$$

The term $J_0$ defines the motor shaft moment of inertia, $x_{m_r} = x + r\cos\phi$ and $y_{m_r} = r\sin\phi$ define the position of the motor unbalanced mass $m_r$ with $r$ been the distance of this mass to the motor center of rotation. Equation 2.2 is rewritten as

$$T = \frac{1}{2}(M + m_r)\dot{x}^2 + \frac{1}{2}(J_0 + m_r r^2)\dot{\phi}^2 - m_r r\dot{x}\dot{\phi}\sin\phi \tag{3}$$

If the gravity potential energy is neglected, then the system's potential energy is simply

$$U = \frac{1}{2}kx^2 \tag{4}$$

## 2.3 *Equations of Motion*

The system equations of motion are obtained by writing the Lagrangian, $L = T - U$, and first-order stationary conditions in the form of Hamilton's equation

$$\frac{d}{dt}\left(\frac{\partial L}{\partial \dot{q}_i}\right) - \left(\frac{\partial L}{\partial q_i}\right) = F_i \tag{5}$$

Where $F_i$ are the non-conservative forces, which are the viscous damping force $F_i = -c\dot{x}$ and the torque $\mathfrak{M}$ applied to the motor.

Applying equations 2.3 and 2.4 into 2.5, it is possible to obtain the cart equation of motion

$$\ddot{x}(M + m_r) + kx + c\dot{x} = m_r r\left(\dot{\phi}^2\cos(\phi) + \ddot{\phi}\sin(\phi)\right) \tag{6}$$

The motion of the motor shaft is given by

$$\ddot{\phi}(J_0 + m_r r^2) = \ddot{x}m_r r\sin(\phi) + \mathfrak{M}(\dot{\phi}) \tag{7}$$

To define a limited power motor, two parameters are used to represent the torque as a function of the angular velocity

$$\mathfrak{M}(\dot{\phi}) = M_0\left(1 - \frac{\dot{\phi}}{\Omega_0}\right) \tag{8}$$

The terms $M_0$ and $\Omega_0$ are constant parameters of the motor which define a limited source of power as the angular velocity increases. This expression defines the characteristic curve of the motor shown in figure 3, where for angular velocities greater than $\Omega_0$ the torque reduces to zero and when the angular velocity is zero, the torque is maximum.

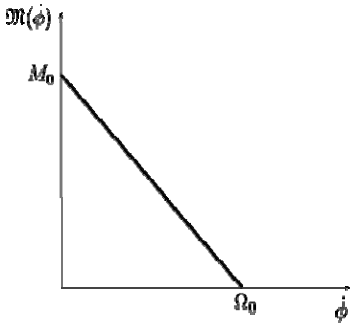


Figure 3. Motor torque characteristic curve.

## 2.4 *Model Order Reduction*

The order of the equations describing the motion of the system (eqs. 2.6 and 2.7) are reduced by the use of the state variables $q_1 = x$, $q_2 = \phi$, $q_3 = \dot{x}$ and $q_4 = \dot{\phi}$, such that, the velocities are re-written as

$$\dot{q}_1 = q_3 \tag{9}$$
$$\dot{q}_2 = q_4 \tag{10}$$

The accelerations can be calculated by solving the linear system of differential equations

$$\begin{bmatrix} (M+m_r) & -m_r r\ \sin(\phi) \\ -m_r r\ \sin(\phi) & (J_0+m_r r^2) \end{bmatrix} \begin{bmatrix} \ddot{x} \\ \ddot{\phi} \end{bmatrix} = \begin{bmatrix} -kx - c\dot{x} + m_r r\dot{\phi}^2 \cos(\phi) \\ \mathfrak{M}(\dot{\phi}) \end{bmatrix} \quad (11)$$

Which gives the following expression for the uncoupled system accelerations ($\dot{q}_3 = \ddot{x}$ and $\dot{q}_4 = \ddot{\phi}$).

$$\dot{q}_3 = \frac{m_r r\left(\mathfrak{M}\sin\phi + \dot{\phi}^2(J_0+m_r r^2)\cos\phi\right)}{M(J_0+m_r r^2) + m\_r(J_0+m_r r^2\cos^2\phi)} - \frac{(J_0+m_r r^2)(kx+c\dot{x})}{M(J_0+m_r r^2) + m\_r(J_0+m_r r^2\cos^2\phi)} \quad (12)$$

$$\dot{q}_4 = \frac{\mathfrak{M}(M+m_r)}{M(J_0+m_r r^2) + m\_r(J_0+m_r r^2\cos^2\phi)} + \frac{m_r r\sin\phi\left(m_r r\dot{\phi}^2\cos\phi - (kx+c\dot{x})\right)}{M(J_0+m_r r^2) + m\_r(J_0+m_r r^2\cos^2\phi)} \quad (13)$$

## 3 MODEL ANALOGY

In this section, an analog model is developed to help understand the dynamic behavior of the system described by the equations developed in the previous section.

When considering a motor mounted over a rigid base, the motor acceleration is defined by

$$\ddot{\phi}(J_0+m_r r^2) = M_0\left(1-\frac{\dot{\phi}}{\Omega_0}\right) \quad (14)$$

It is possible to develop a model analogy for the system described in equation 14 using the system shown in figure 4. In this figure, a wheel must climb a ramp to reach a certain level of energy defined by $\Omega_0$. For a motor with no resistive torque ($\mathfrak{M} = M_0$) the angular acceleration is constant and therefore, the angular velocity of the wheel increases by a constant rate. The slope of the ramp can be related to the motor inertia defining the rate which the angular velocity increases. The motor torque should be switched off as the desired angular velocity $\Omega_0$ is achieved.

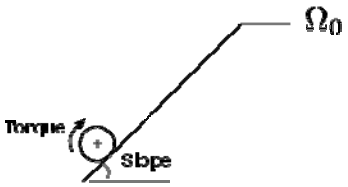


Figure 4. Analogy by a wheel climbing a ramp (no resistive torque)

When considering a motor with resistive torque, the angular acceleration is no longer constant and decreases as the angular velocity increases. The system shown in figure 5 is used to represent the motor with resistive torque, where it is more difficult to reach the energy level $\Omega_0$ and the rate of changing the velocity is no longer linear.

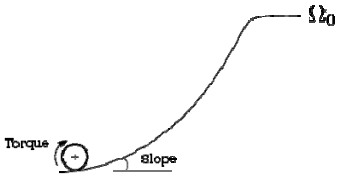


Figure 5. Analogy by a wheel climbing a ramp (with resistive torque)

When the motor is mounted on a flexible base, it is clear in equation 13 that the angular acceleration is also a function of the cart motion. Also, the motion of the cart is a function of the acceleration and angular velocity of the motor.

The system shown in figure 6 represents an analogy when the motor is mounted on a flexible base. Similarly to figures 4 and 5, a wheel must climb a ramp to reach the level of energy defined by $\Omega_0$. In this case, the ramp path is modified by the cart resonance frequency $\omega_0$. The resonance frequency is represented by the valley in the ramp path. The deep and the width of the valley in the ramp is related to the amplitude of the motion of the cart and in some cases the wheel can get stuck inside the valley in the ramp path. The dynamic factors controlling this behavior are explored in the following sections of this paper.

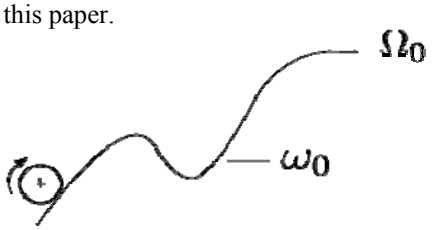


Figure 6. Analogy of the resonance frequency in the ramp path

## 4 NUMERICAL SIMULATIONS

In this section numerical simulations are performed with the system defined by the first order differential equations developed in the previous sections. The parameters used in the simulations are defined in the table 1 which are approximated values of the physical system discussed in the section 5.

Table 1. System Nominal Parameters.

| Parameter | Value |
|---|---|
| Cart Mass $M$ | 0.064 kg |
| Unbalanced Mass $m_r$ | 0.0021 kg |
| Stiffness $k$ | 142.27 N/m |
| Damping Coefficient $c$ | 0.01 Ns/m |
| Shaft Inertia $J_0$ | $1 \times 10^{-7}$ Nm$^2$ |
| Unbalanced radius $r$ | 0.003 m |
| Motor Constant $M_0$ | $1 \times 10^{-5}$ Nm |

### *4.1 Model Implementation*

The numerical model was implemented using GNU Octave and C language using the GSL (GNU Scientific Library for numerical integration). Both GNU Octave and GSL are freely available.

Two different numerical integration algorithms were used. The first is the well-known explicit Runge-Kutta method of order (4,5) used for non-stiff ordinary differential equations. The second is the 5-th order algorithm for stiff ordinary differential equations described in reference [8]. The parameters which are of interest in the simulations are the cart displacement (or velocity) and the motor angular velocity. The motor angular position is a parameter that is confined in the range 0-2π.

### 4.2 *Stationary Conditions*

This numerical example considers the case of setting the motor angular velocity to a fixed value. The motor is accelerated from rest to a fixed velocity by changing the parameter $\Omega_0$ The simulations where performed for frequencies around the cart resonance frequency ( $\Omega_0$ and are presented in figures 7 and 8.

Figure 7 shows that when $\Omega_0$ is slightly bigger than $\Omega_0$ the angular velocity does not increase.

For instance, when setting $\Omega_0 = 1.1$ the motor does not reach the angular velocity $1.1\Omega_0$, instead it will oscillate with angular velocity $\Omega_0$. The consequence is that this energy is transferred to cart displacement amplitude.

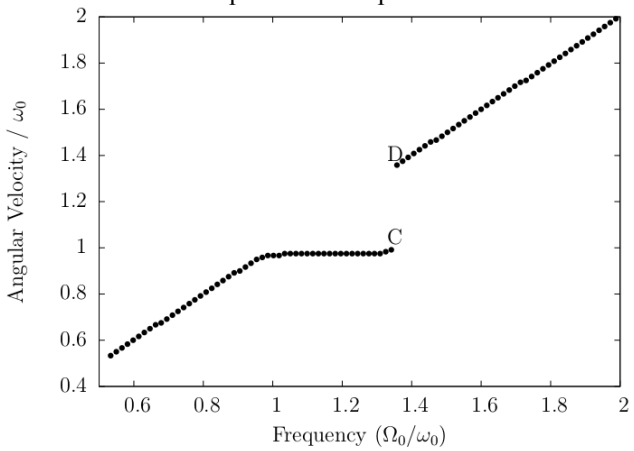


Figure 7. Angular Velocity as a function of $\Omega_0$

The cart RMS (root mean square) magnitude of the acceleration was plotted in figure 8 as a function of the oscillation frequency as the parameter $\Omega_0$increases.

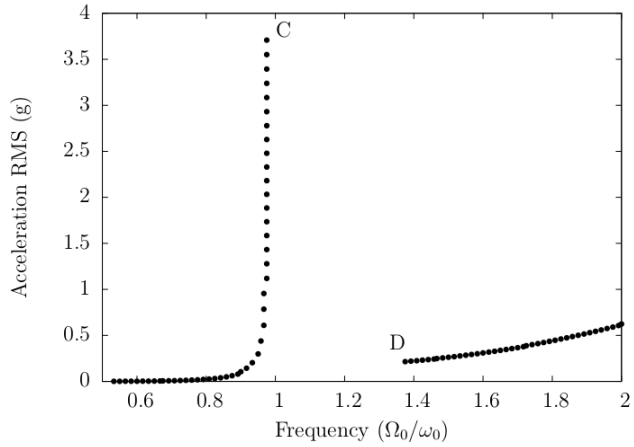


Figure 8. Root Mean Square Acceleration as a function of the Oscillation Frequency

It is possible to note in 7 and 8 a region between C and D with no data points. This region corresponds to a jump phenomenon described previously by Sommerfeld.

### 4.3 *Non Stationary Conditions*

The acceleration profile for the motor operation of coast up can be obtained by setting the variable $\Omega_0$ time dependent as follows

$$\Omega_0(t) = \frac{\Omega_2 - \Omega_1}{t_2} t \tag{15}$$

where, $\Omega_2$ is the desired final angular velocity, $\Omega_1$ is the initial angular velocity, $t_2$ is the amount of time to accelerate from $\Omega_1$ to $\Omega_2$ and $t$ is the instant time. The torque applied to the motor is then defined as

$$\mathfrak{M}(\phi) = M_0 \left( \dot{1} - \frac{\dot{\phi}}{\Omega_0(t)} \right) \tag{16}$$

The typical results obtained in these simulations are illustrated in figures 9 and 10. The vertical axis of figure 9 shows the angular velocity of the motor normalized by the cart resonance frequency $\Omega_0$. The two curves in this figure show two situations when passing through the cart resonance frequency. The ticker line indicates the case of resonance capture and the thin line is the case of no resonance capture. The correspondent cart displacements curves are shown in figure 10. In the case of resonance capture (Sommerfeld effect) the cart displacement amplitude increases and the motor angular velocity varies around the cart resonance frequency $\Omega_0$.

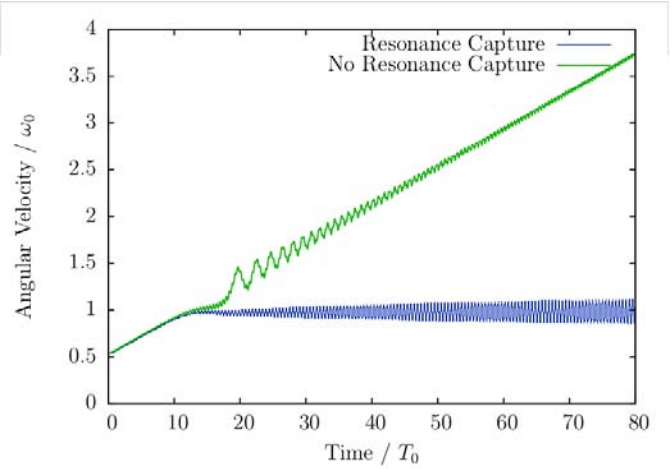


Figure 9. Angular velocity for the cases with Resonance Capture and No Resonance Capture

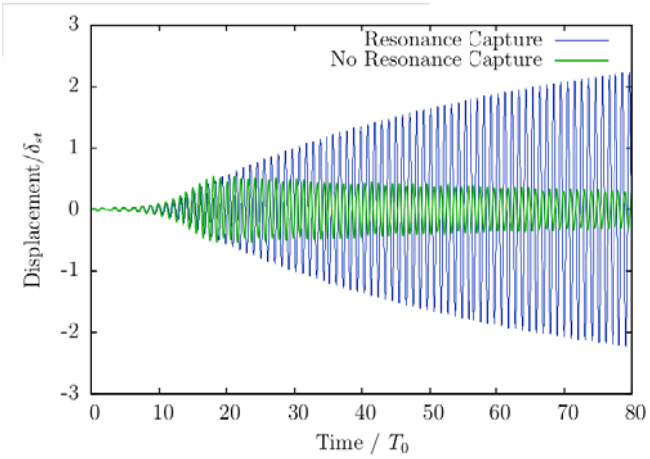


Figure 10. Displacement amplitude for the cases with resonance capture and no resonance capture

## 5 EXPERIMENTAL TESTS

This section explains the experimental procedure used to verify some of the characteristics investigated by the numerical model studied in this work. The experiment consisted of measuring acceleration in the tip of a cantilever beam using an excitation produced by an unbalanced DC motor positioned in the free end. Figure 7 shows a picture of the experiment

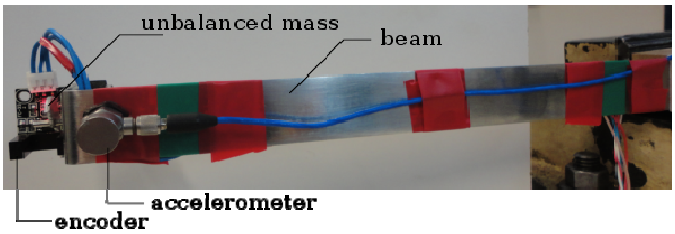


Figure 11. Clamped beam and experimental apparatus used in the experiment.

An encoder device was built to measure the rotating frequency of the DC motor. The motor rotating frequency was obtained using an Arduino One microcontroller. The voltage applied to the motor was also controlled by the microcontroller. To measure the vibration an accelerometer with nominal sensitivity of 100 mV/g was used and connected to Digital Acquisition System. The mass of the encoder, the mass of the accelerometer and the armature mass of the DC motor are represented by the mass $M_c$ shown in figure 1.

The experimental procedure consisted of slow increasing/decreasing various steps of voltage applied to the DC motor in order to identify the Sommerfeld effect observed in the numerical simulations. The results are presented in figures 12 and 13.

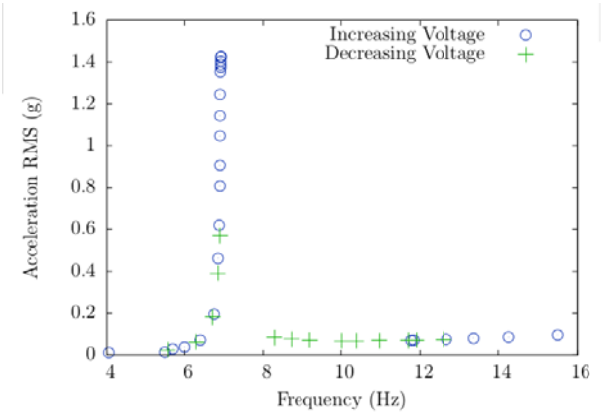


Figure 12. Root mean square amplitude of the beam tip as a function of the unbalanced mass rotation frequency.

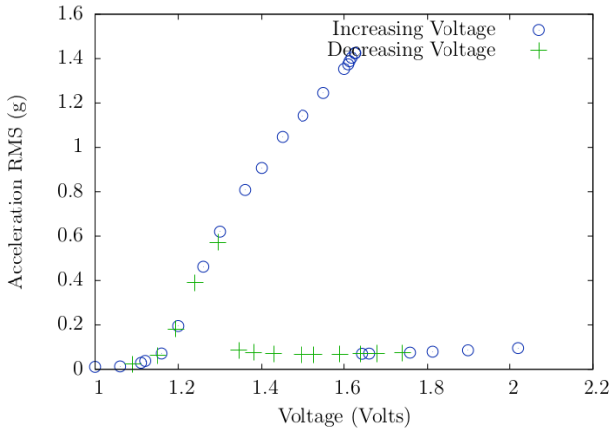


Figure 13. Root mean square amplitude of the beam tip as a function of the voltage applied to the motor.

## 6 CONCLUSIONS

A simplified numerical model of a cantilever beam coupled with an unbalanced DC motor has been presented. The model presents the condition of resonance capture known as Sommerfeld Effect. The model has been validated with experiment tests which show the resonance capture effect.

## REFERENCES

[1] Balthazar, J.M., et al., *An overview on non-ideal vibrations.* Meccanica, 2003. **38**(6): p. 613-621.

[2] Sommerfeled, A., *Beitrage zum dynamischen Ausbau der Festigkeitslehre.* Physikalische Zeitschrift, 1902. **12**: p. 13.

[3] Cvetićanin, L., *Dynamics of the non-ideal mechanical systems: A review.* Journal of the Serbian Society for Computational Mechanics/Vol, 2010. **4**(2): p. 75-86.

[4] Eckert, M., *DerSommerfeld-Effekt': Theorie und Geschichte eines bemerkenswerten ResonanzphÃ¤nomens.* European Journal of Physics, 1996. **17**(5): p. 285.

[5] Blekhman, II, D.A. Indeitsev, and A.L. Fradkov, *Slow motions in systems with inertial excitation of vibrations.* Journal of Machinery Manufacture and Reliability, 2008. **37**(1): p. 21-27.

[6] Dimentberg, M.F., et al., *Dynamics of an unbalanced shaft interacting with a limited power supply.* Nonlinear Dynamics, 1997. **13**(2): p. 171-187.

[7] Harris, C.M. and A.G. Piersol, *Harris' shock and vibration handbook*. Vol. 5. 2002: McGraw-Hill New York.

[8] Wanner, G. and E. Hairer, *Solving Ordinary Differential Equations II*. Vol. 1. 1991: Springer-Verlag, Berlin.